JOURNAL OF MATERIALS SCIENCE 26 (1991) 6650–6654

Role of vacancies and implantation defects in GaAs/AlAs superlattice intermixing

S. MITRA
Materials Science Group, Mechanical Engineering, Naval Postgraduate School, Monterey, CA 93943, USA

J. P. STARK
Center for Materials Science and Engineering, University of Texas at Austin, Austin, Texas 78712, USA

Ga/Al intermixing in GaAs/AlAs superlattice (SL) structures is studied in the presence of an epitaxially grown dopant (Si) with and without the aid of vacancies. Rapid thermal annealing (900 °C/20 min) after growth is insufficient to induce intermixing without the presence of excess vacancies as observed by Auger electron spectroscopy in conjunction with Ar ion sputtering. Vacancies themselves also enhance the intermixing process, and their role is explained with the recently proposed two-atom ring mechanism of diffusion. The effect of medium dose medium energy Be implantation into the SL is also studied using cross sectional transmission electron microscopy (XTEM). Two types of damage are observed, twins when liquid nitrogen (LN_2) is used to cool the sample holder chamber, and high dislocation densities at room temperature conditions. Rapid thermal annealing effectively removes the twins but gives heavy intermixing in the case of the dislocation networks.

1. Introduction

Various investigators have studied the phenomenon of enhanced intermixing of Ga and Al in the $Al_xGa_{1-x}As$ system, in the presence of dopants like Zn [1, 2], Si [3, 4, 5] and Be [6, 7]. Chang and Koma [8] found that intermixing of Ga and Al in AlAs–GaAs superlattices in the absence of dopants was very slow, about 8×10^{-18} cm^2 s^{-1} at 1000 °C. A number of mechanisms have been proposed to explain the enhancement effect of dopants on the intermixing process. These include: group III sublattice vacancy diffusion [8], the As divacancy model [9], the Fermi level model [10], and the recently proposed model of a two-atom ring mechanism of exchange on the group III sublattice [11, 12]. This study investigates the application of the two-atom ring mechanism and establishes the role of vacancies in the dopant diffusion and intermixing processes. It will be shown that the presence of vacancies can lead to intermixing in two ways: (i) by aiding dopant diffusion which can then enhance intermixing through the ring mechanism, and (ii) by themselves being responsible for enhanced group III sublattice activity. A vacancy-lattice atom ring exchange is proposed and the theoretical activation energies calculated for this diffusion model [12] agree well with the self diffusion activation energies measured for Ga in GaAs.

Ion implantation into GaAs is often preferably done into an "amorphous" surface layer [13]. This gives a better Gaussian distribution of dopant concentrations, especially when shallow layers are sought. Some authors [14, 15] have shown that high dose implantation of Be into GaAs gives tails in the concentration profile. This necessitates the use of the amorphous state, which can also be used to isolate devices since the heavily damages layer is rendered semi-insulating [16]. Instead of using high doses, known to give dopant redistribution on annealing, medium doses and low substrate temperatures are used here. Furthermore, the added complexity of interfaces has been introduced by implanting into superlattices. To study the effect of temperature, implantation is also done at room temperature conditions.

The effect of rapid thermal annealing on the implantation defects is investigated by annealing both structures. The higher temperature defect (dislocation loops) is found to enhance intermixing, while the low temperature defect (twins), is removed by annealing, without any intermixing taking place.

2. Experimental details

The GaAs/AlAs structures are grown by molecular beam epitaxy on a semi-insulating GaAs substrate with (1 0 0) orientation and at substrate temperatures of 650 °C. The structure is shown in Table I. Layer no. 5 is doped with Si to a concentration of 5×10^{18} cm^{-3}, theoretically enough to cause intermixing to begin under annealing temperatures in excess of 800 °C [3]. Different thicknesses of GaAs are grown to check for any thickness effects on the intermixing.

0022–2461/91 $03.00 + .12

TABLE I Structure of the superlattice grown by MBE

Layer no.	Composition	Thickness (nm)	Layer no.	Composition	Thickness (nm)
1	AlAs	30	9	AlAs	30
2	GaAs	30	10	GaAs	10
3	AlAs	30	11	AlAs	30
4	GaAs	15	12	GaAs	8
5 Si doped	AlAs	30	13	AlAs	30
6	GaAs	10	14	GaAs	5
7 Be implant	AlAs	30	15	AlAs	30
8	GaAs	13	16	GaAs	150

The as grown superlattice is then analysed in a Physical Electronics SAM 590 Auger electron microprobe equipped with Ar ion sputtering facilities. The depth profile of the Ga (1070 eV) peak is followed for both an as grown and an annealed sample. Rapid thermal annealing, at 900 °C for 20 min, is done in a slowly flowing atmosphere of forming gas with total face to face contact with another GaAs cap piece to provide the necessary As overpressure needed in the equivalent open tube annealing configurations. Two other samples are annealed at 850 °C for 10 min, but with the GaAs cap 70% on and 20% on, respectively. In the absence of the necessary overpressure, As and Ga vacancies are introduced and the effects of these on intermixing can be studied by depth profiling techniques.

The SL is also implanted with Be ions (dose 1×10^{14} cm^{-2} at 100 keV). These medium dose medium energy implants are done at two different temperatures. Standard range analysis [17] gives the projected range as 320 nm and the straggle as 140 nm in bulk GaAs. Samples used in this study are GaAs/AlAs superlattices with the added parameters of interfaces and temperature, and the range values are thus only approximate. Be is implanted at two different temperature conditions and the damage studied by cross sectional transmission electron microscopy (XTEM). In one case the sample holder chamber is cooled to liquid nitrogen (LN_2) temperatures (standard practice for implantation into Si). The sample, however, does not go down to LN_2 temperatures. Furthermore there is no sample temperature measuring device in use consequently preventing accurate determination of actual target temperature. The other condition of implantation is under room temperature. XTEM samples are prepared usng M610 adhesive and ion milling techniques. A JEOL 200CX transmission electron microscope is used to observe the interfaces in the SL. Implanted samples are also annealed (RTA at 850 °C for 10 min) and the diffusion activity is studied using AES depth profiling.

3. Results and discussion

3.1. Role of vacancies (unimplanted samples)

The as-grown and annealed Ga peak to peak height depth profiles are shown in Fig. 1. The Si doping clearly does not have any effect on the intermixing at the concentration level of 5×10^{18} cm^{-3} for anneals of 900 °C for 20 min. Although literature values [18] of

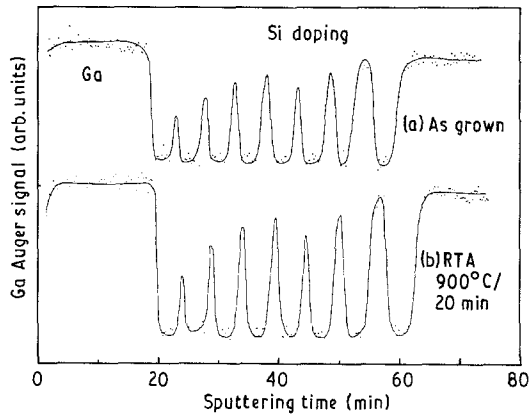

Figure 1 AES depth profile of the (a) as grown and (b) annealed SL (900 °C/20 min, with 100% face-to-face coverage).

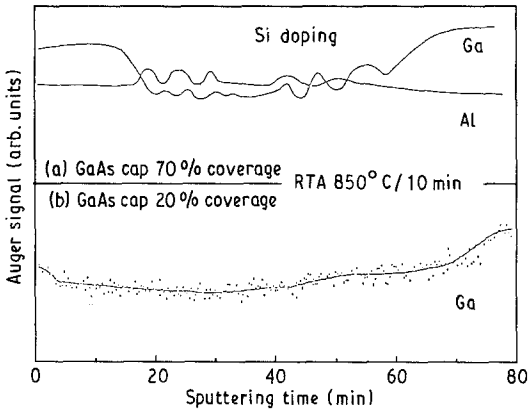

Figure 2 AES depth profile of the annealed SL (850 °C/10 min), with (a) 70% and (b) 20% coverage, showing intermixing.

5×10^{18} cm^{-3} appear to be sufficient to induce intermixing, the effect was obtained after annealing at 800 °C for 2 h, and was only partial. Implanted Si gave a more pronounced intermixing effect as is expected [4]. Fig. 2 shows the depth profiles of the samples annealed with incomplete As overpressures. The select point of the depth profiling is chosen to lie under the covered regions for both samples. The slightly exposed sample shows distinct intermixing in the region of Si doping, with intermixing progressing towards the surface, the source of vacancies.

Inadequate overpressures give rise to both As and Ga vacancies, and Chiang and Pearson [19] have established that the As vacancy concentration is at least one order of magnitude greater than $[V_{Ga}]$. Also,

the (V_{As}) diffusivity is high enough to give a flat profile inside the SL. Vacancy formation in GaAs follows the relations:

$$As_{As} = 1/2\,As_2(g) + V_{As} \quad (1)$$

$$1/2\,As_2 = As_{As} + V_{Ga} \quad (2)$$

Chiang and Pearson [19] have measured the diffusivities as

$$D(V_{Ga}) = 2.1 \times 10^{-3} \exp[-2.1/kT] \quad (3)$$

$$D(V_{As}) = 7.9 \times 10^{3} \exp[-0.4/kT] \quad (4)$$

Ga and As vacancies created at the exposed surface diffuse down and laterally to aid Si diffusion.

Si can diffuse by the Greiner-Gibbons mechanism [20] of vacancy assisted Si pair movement. This process needs both As and Ga vacancies and is controlled by the [V_{Ga}] concentration. The diffusing Si can effect the group III sublattice intermixing by reducing the activation barrier for the ring exchange mechanism to interchange sites 1 and 2 in Fig. 3. This model has been published elsewhere [11].

Furthermore it is proposed that the diffusion of vacancies from the surface to the Si takes place by a "vacancy-lattice atom" ring exchange. Here the activation energy is calculated by taking the difference in energy between the activated state and the ground state of a Ga atom. The energies obtained for this ring exchange (essentially self-diffusion of Ga in GaAs), agree well with measured activation energies and will be published later [12].

3.2. High vacancy concentration

From Fig. 2b, a high vacancy concentration is found to drastically increase intermixing. A mechanism to explain this effect is proposed here. In the literature [19] it has been shown that V_{As}^{+} acts as a donor and V_{Ga}^{-} as an acceptor. Individually V_{As}^{+} can effectively decrease the activation barrier for sites 1 and 2 in Fig. 4 to exchange places by distorting the lattice through ionic-like interactions. This effect is not as pronounced as silicon's, since electron screening effects of ion cores need to be incorporated in the magnitude of the deviating force. At high vacancy concentrations however, V_{As}^{+} and V_{Ga}^{-} can form pairs (V_{As}^{+}–V_{Ga}^{-}). V_{Ga}^{-} in the pair can now further decrease the activation barrier for 1–2 exchange by displacing As^{+} on sites 3 and 4 in other directions. This effect is stronger since the V_{Ga}^{-} is closer to sites 3 and 4, thus facilitating site exchange of site 1 and the next nearest neighbor on the Ga sublattice in the neighboring unit cell, originally blocked by As at site 4.

Finally, the intermixing effect of activation barrier reduction is more pronounced than the ring diffusion mechanism of vacancy assisted self diffusion and explains the Si and excess vacancy effects on the SL.

3.3. Implanted samples

The brightfield cross-sectional TEM micrograph of the low temperature implanted SL is shown in Fig. 5. The corresponding diffraction pattern is shown in Fig. 6. Evidence of extra spots is clearly visible around the 400, 800 and $\bar{1}\,1\,\bar{1}$ spots. According to Pashley and Stowell [21], fcc lattices have extra twinning spots in their reciprocal lattices, due to twinning, along the $\langle 1\,1\,1 \rangle$ directions in reciprocal space. This matches well with the extra spots for a beam direction of $[0\,\bar{1}\,\bar{1}]$ in Fig. 6. These twins run through the entire superlattice from the top of the GaAs cap to the first epitaxially grown layer, but do not enter the substrate. Other implanted samples also show twinning while the as grown sample has no evidence of twinning.

The brightfield cross-sectional TEM micrograph of the room temperature implanted SL is shown in Fig. 7. Here a high density of dislocation loops can be seen in the first AlAs layer, essentially originating from the

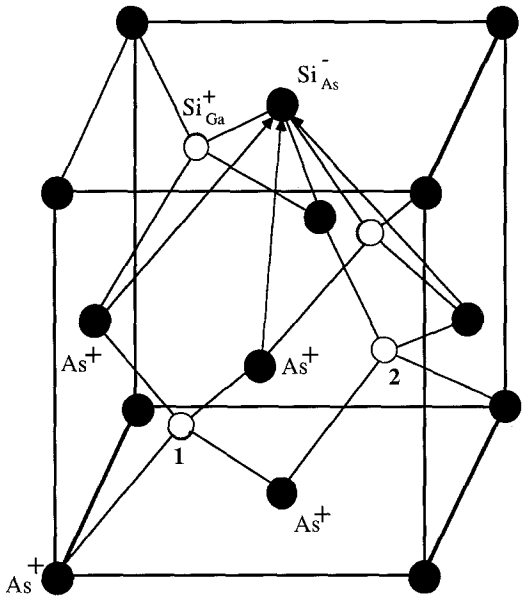

Figure 3 Si donor-acceptor pair in a GaAs unit cell facilitating group III sublattice exchange.

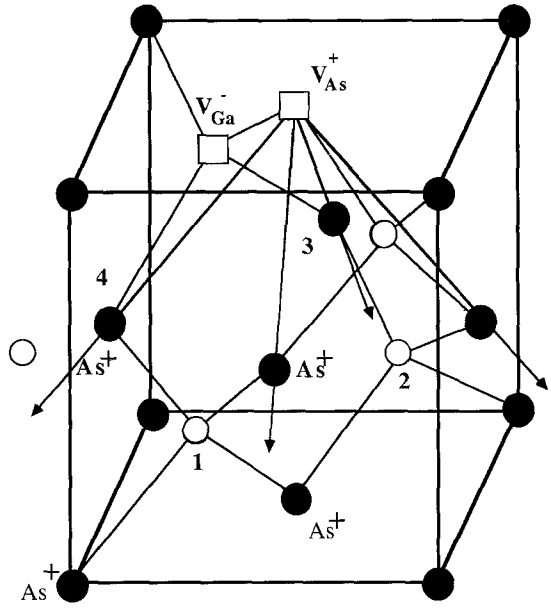

Figure 4 (V_{As}^{+}–V_{Ga}^{-}) pair facilitating group III sublattice exchange in a GaAs unit cell.

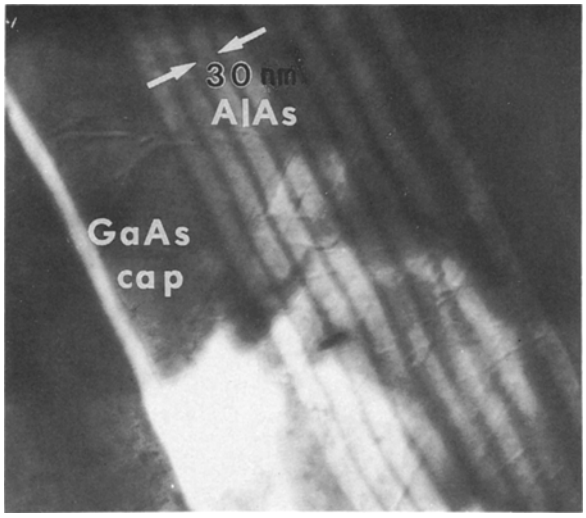

Figure 5 Brightfield XTEM micrograph of Be implanted SL showing twins (low temperature conditions).

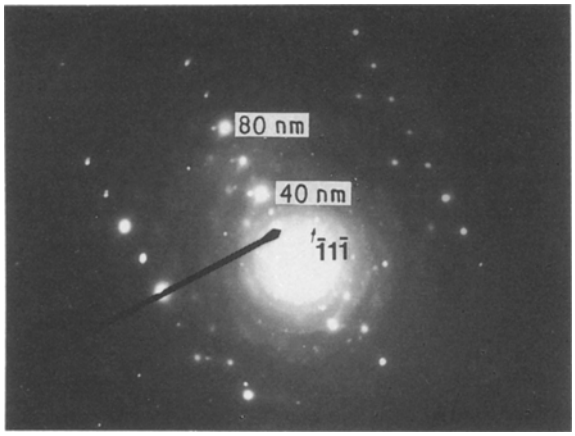

Figure 6 Diffraction pattern of Fig. 5 showing extra spots due to twinning.

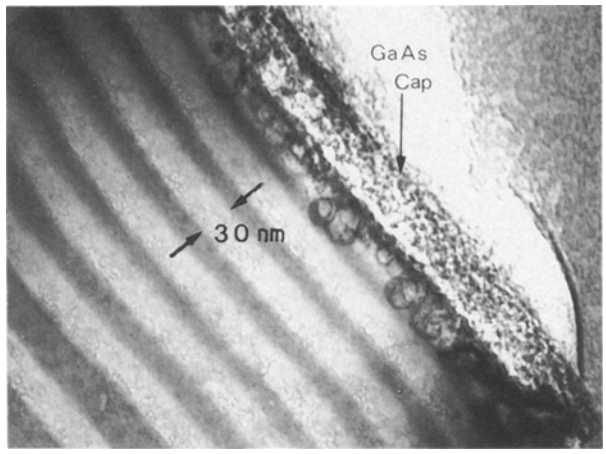

Figure 7 Brightfield XTEM micrograph of Be implanted SL showing dislocation networks (room temperature conditions).

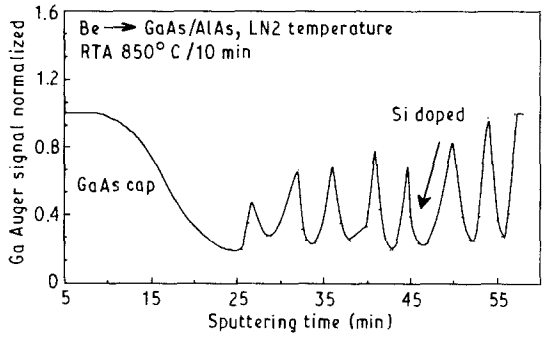

Figure 8 Typical AES depth profile of room temperature implanted and annealed SL showing intermixing at the damaged region only.

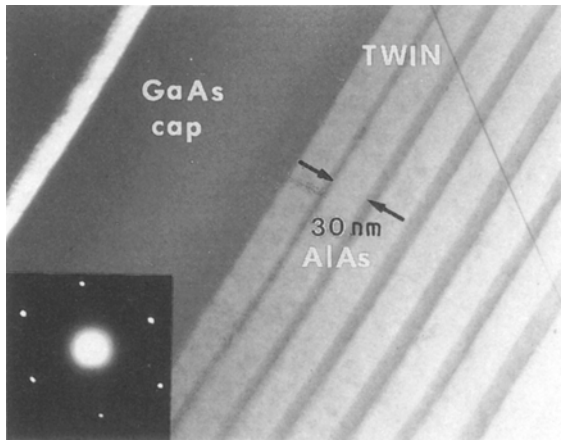

Figure 9 Brightfield XTEM micrograph of annealed SL from Fig. 5. Isolated twin visible.

first interface that the implanted ions encounter. The dislocation network is clearest at incident beam direction of [0 1 2]. Although the cap layer of GaAs is partially destroyed during sample preparation, it can be seen that the damage is confined to the cap layer and the first AlAs layer.

Another interesting feature in Fig. 7 is the slight damage (dislocations), found at the bottom of each AlAs layer. This is introduced during the growth process and can be removed by annealing as will be shown later.

To evaluate the effect of this damage on the intermixing, RTA (850 °C/10 min/total top face coverage) is done on the implanted samples. Fig. 8 shows a typical AES depth profile of the annealed, room temperature implanted sample. Interdiffusion is clearly visible near the cap layer, as expected. The twinned sample is also annealed (RTA/850 °C/10 min/total top face coverage), but the AES depth profile does not show any intermixing. XTEM observations of the twinned and annealed sample (at similar orientations) show almost no more twins as seen in Fig. 9, with the corresponding diffraction pattern inset. The interfaces are straightened out considerably (as with the dislocated sample), and very few isolated twins remain (feature in Fig. 9). Also the slight damage seen in the AlAs layers due to growth has been annealed out.

Finally, since the maximum Be concentration in this zone (assuming a Gaussian distribution after

implantation) is $1 \times 10^{18}\,cm^{-3}$, no Be induced enhancement has taken place (below the Be threshold in [7] Fig. 1).

4. Conclusions

Medium dose medium energy implants into GaAs at room temperature give damage concentration at the first interface encountered. This damage takes the form of a dense dislocation network to the extent of rendering the top layer "amorphous". Subsequent annealing will seriously degrade the SL by interdiffusion at the dislocation regions. Room temperature implants of this sort (into superlattices) are thus unsuitable for isolating devices and ensuring well behaved shallow doping profiles as the effect of interfaces needs to be taken into consideration.

Low temperature implants gave twins that could be effectively removed by annealing, without intermixing taking place. These are due to the superlattice itself as no twins are reported due to implantation in bulk GaAs. The twins run across the (1 1 1) planes and are not involved with enhancement of the diffusion process.

It is shown that vacancies play a role in the diffusion of the dopant Si, but not in the group III intermixing process at low vacancy concentrations. When $[V_{As}]$ and $[V_{Ga}]$ concentrations are large enough, as obtained by annealing with insufficient As overpressure, vacancy pairs can form: $(V_{As}^{+}-V_{Ga}^{-})$. These pairs can reduce the activation barrier for the ring exchange mechanism to become operative and give intermixing on the group III sublattice.

Vacancies also aid the diffusion of Si by previously established mechanisms, but the intermixing effects of Si can only be realized by the ring exchange mechanism being the operative diffusion mechanism. This reasoning is further emphasized by the relatively open structure of the diamond cubic lattice which facilitates the movement of atoms by a ring mechanism.

References

1. J. W. LEE and W. D. LAIDIG, *J Electron Mater.* **13** (1984) 147.
2. W. D. LAIDIG, N. HOLONYAK Jr., M. D. CAMRAS, K. HESS, J. J. COLEMAN, P. D. DAPKUS and J. BARDEEN, *Appl. Phys. Lett.* **38** (1981) 776.
3. M. KAWABE, N. MATSURA, N. SHIMIZU, F. HASEGAWA and Y. NANNICHI, *Jpn J. Appl. Phys.* **23** (1984) L623.
4. J. J. COLEMAN, P. D. DAPKUS, C. G. KIRKPATRICK, M. D. CAMRAS and N. HOLONYAK Jr., *Appl. Phys. Lett.* **40** (1982) 904.
5. K. MEEHAN, P. GAVRILOVIC, N. HOLONYAK Jr., R. D. BURNHAM and R. THORNTON, *ibid.* **46** (1985) 75.
6. D. R. MYERS, R. M. BIEFELD, I. J. FRITZ, S. T. PICRAUX and T. E. ZIPPERIAN, *ibid.* **44** (1984) 1052.
7. M. KAWABE, N. SHIMIZU, F. HASEGAWA and Y. NANNICHI, *ibid.* **46** (1985) 849.
8. L. L. CHANG and A. KOMA, *ibid.* **29** (1976) 138.
9. V. S. LYONS, *J. Phys. Chem.* **63** (1959) 1142.
10. T. Y. TAN and U. GÖSELE, *J. Appl. Phys.* **61[5]** (1987) 1843.
11. S. R. TATTI, S. MITRA and J. P. STARK, *ibid.* **65[6]** (1989) 2547.
12. S. MITRA and J. P. STARK, unpublished work.
13. S. K. GHANDHI, "VLSI Fabrication Principles" (Wiley and Sons, New York, 1983).
14. J. COMAS and L. PLEW, *J. Elect. Mater.* **5** (1976) 209.
15. S. NOJIMA and Y. KAWASAKI, *Jpn J. Appl. Phys.* **17** (1978) 1845.
16. A. G. FOYT, W. T. LINDLEY, C. M. WOLFE and J. P. DONNELLY, *Solid State Electron.* **12** (1969) 209.
17. J. LINDHARD, M. SCHARFF and H. E. SHIØTT, *Mat. Fys. Medd. Dan. Vidensk. Selsk.* **33[14]** (1963) 1.
18. K. MATSUI, J. KOBAYASHI, T. FUKUNAGA, K. ISHIDA and H. NAKASHIMA, *Jpn. J. Appl. Phys.* **25** (1986) L651.
19. S. Y. CHIANG and G. L. PEARSON, *J. Appl. Phys.* **46[7]** (1975) 2986.
20. M. E. GREINER and J. F. GIBBONS, *ibid.* **57[12]** (1985) 5181.
21. D. W. PASHLEY and M. J. STOWELL, *Phil. Mag.* **8** (1963) 1605.

Received 7 March
and accepted 3 December 1990